Modeling Gas Effects in a Bubbling Fluidized Bed Reactor for Biomass Pyrolysis

Gavin M. Wiggins, ??

July 13, 2020

Contents

1	Inti	roduction	2
2	Exp	perimental apparatus	2
3	Mo	deling approach	4
	3.1	Gas properties	4
	3.2	Fluidization correlations	5
	3.3	Pyrolysis kinetics	5
	3.4	Parameters	
	3.5	Simulation cases	7
4	Res	sults and discussion	8
	4.1	Comparison of gas properties	8
	4.2	Fluidization effects	
	4.3	Evaluation of the kinetic scheme	10
	4.4	Solid and gas residence times	12
5	Cor	nclusion	12
6	Sou	rce code	12

Abstract

Fast pyrolysis of biomass in a fluidized bed reactor is typically conducted in a nitrogen gas environment. Recycling product gas can improve the economics of operating such a system by reducing reliance on pure process streams.

1 Introduction

Fast pyrolysis is a versatile method for thermochemical conversion of solid biomass into liquid bio-oil which can be used for bio-fuel and high-value chemical production. Bio-oil is commonly generated in bubbling fluidized bed and circulating fluidized bed reactor systems in which biomass particles rapidly devolatilize in the absence of oxygen into mixtures of light gases, condensable bio-oil vapors, and solid char [4, 5, 12]. Since biomass pyrolysis normally occurs in a non-oxidizing environment, the fluidization gas (carrier gas) is often pure nitrogen [12]. To maximize bio-oil yields, the reactor typically operates at temperatures near 500°C and must maintain particle residence times up to 10 seconds and gas residence times less than 2 seconds [5]. Deviations from these conditions can result in significant production and quality penalties, therefore optimal reactor design and control become crucial to achieving commercially viable bio-oil production.

To improve the economic possibilities of biomass fast pyrolysis systems, char can be burned for process heat while recycled pyrolysis gas can assist with fluidization [4, 10]. The major generated components of pyrolysis gas are CO, CO₂, CH₄, H₂, and other light hydrocarbons [1, 16]. Several experiments investigated the effects of these gases on reactor conditions and pyrolysis yields [10, 13, 16] but modeling the effects of the different gases was not discussed.

There are several models available that investigate the hydrodynamics and conversion of biomass at fast pyrolysis conditions in fluidized bed reactors [14, 11]. As is typical for biomass pyrolysis, these models assume the fluidization gas is pure nitrogen. The authors are not aware of any published models in the biomass pyrolysis literature that account for the effects of fluidization or carrier gas other than nitrogen.

This paper uses engineering correlations, reduced-order modeling techniques, and CFD simulations to investigate the effects of gas mixtures in a fluidized bed biomass pyrolysis reactor. The scope of this study is to evaluate different gas mixtures and there effects on the hydrodynamics and biomass conversion in fluidized bed reactors operating at fast pyrolysis conditions.

2 Experimental apparatus

The NREL 2FBR reactor system thermochemically converts biomass feedstock at fast pyrolysis conditions. The system is comprised of two bubbling fluidized bed (BFB) reactors where the first reactor is for biomass fast pyrolysis and the second reactor is for vapor phase upgrading. Modeling activities discussed in this paper refer to the BFB pyrolysis reactor.

An overview of the NREL 2FBR system is shown in Figure 1, components of the pyrolysis reactor are detailed in Figure 2, while dimensions and typical operating conditions of the pyrolysis unit are given in Figure 3. Sand is used as the dominant heat transfer medium in the pyrolyzer. Biomass particles are fed to the reactor via a screw auger and nitrogen is used as the fluidization/carrier

gas. More information about the NREL 2FBR biomass pyrolysis system is available elsewhere $[8,\,15].$

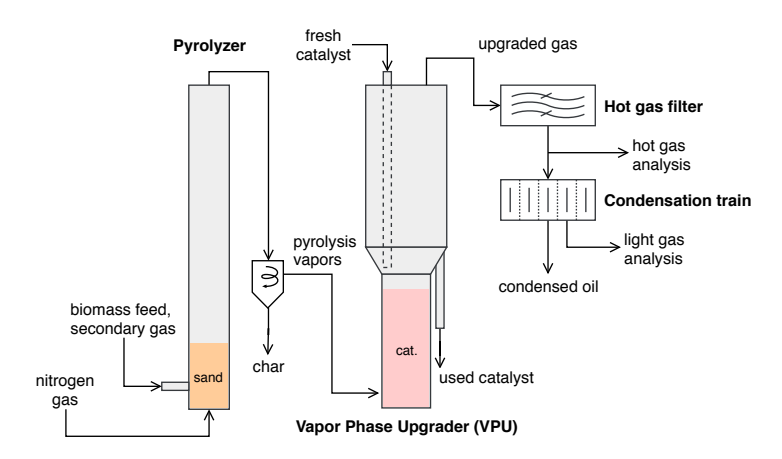


Figure 1: Overview of the NREL 2FBR system. Biomass fast pyrolysis occurs in the pyrolyzer (left) and gaseous products are catalytically upgraded in the vapor phase upgrader (right).

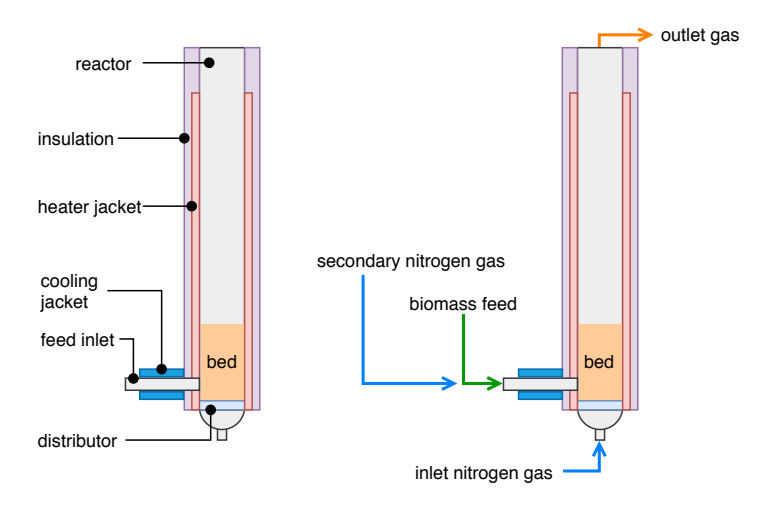


Figure 2: Components of the BFB biomass pyrolysis reactor referred to as the "pyrolyzer" in the NREL 2FBR system.

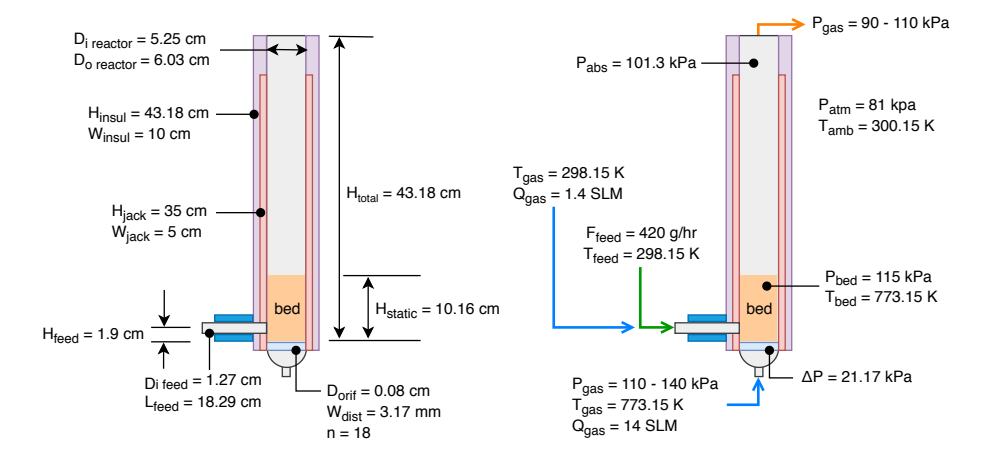


Figure 3: Dimensions and typical fast pyrolysis operating conditions for the BFB biomass pyrolysis reactor in the NREL 2FBR system.

3 Modeling approach

Engineering correlations, reduced-order models, and CFD modeling techniques were used to investigate the effects of recycled gas on the operation of a fluidized-bed biomass pyrolysis reactor. The following sections discuss approaches implemented in this work for calculating gas properties and the associated effects on fluidization conditions and pyrolysis yields.

3.1 Gas properties

Density (kg/m³) of an individual gas is calculated from the ideal gas law

$$\rho_{gas} = \frac{PM}{RT} \tag{1}$$

where P is pressure (Pa), M is molecular weight (g/mol), R is the gas constant [(m³ Pa) / (K mol)], and T is temperature (K). Gas viscosity (μ P) is given as

$$\mu_{gas} = A + BT + CT^2 + DT^3 \tag{2}$$

where coefficients A, B, C, and D are obtained for a given gas from tables in Yaws' Handbook and T is gas temperature (K). Thermal conductivity (k) of the gas is given as

$$k_{gas} = A + BT + CT^2 + DT^3 (3)$$

where coefficients A, B, C, and D are also from the Yaws' Handbook and T is again the gas temperature (K).

Several methods are available to calculate the viscosity of a gas mixture. Equation 4 calculates the mixture viscosity from the sum of the mole fraction

and viscosity product of each gas component in the mixture [6] while Equation 5 accounts for the molecular weight of each gas component [7].

$$\mu_{mix} = \sum (x_i \cdot \mu_i) \tag{4}$$

$$\mu_{mix} = \frac{\sum (\mu_i \cdot x_i \cdot \sqrt{MW_i})}{\sum (x_i \cdot \sqrt{MW_i})}$$
 (5)

3.2 Fluidization correlations

For a bed of particles, the minimum fluidization velocity U_{mf} is the gas velocity at which the drag force of the upward moving gas equals the weight of the particles. Kunii and Levenspiel [9] provide the following equation for calculating minimum fluidization velocity

$$U_{mf} = \frac{Re_{p,mf}\mu}{d_p\rho_q} \tag{6}$$

where μ is gas viscosity (kg/ms), d_p is particle diameter (m), ρ_g is gas density (kg/m³), and $Re_{p,mf}$ is the particle Reynolds number (-) at minimum fluidization conditions.

The Reynolds number is calculated from the Archimedes number (Ar) and two dimensionless constants (a, b) which represent experimental coefficients.

$$Re_{p,mf} = (a^2 + bAr)^{1/2} - a$$
 (7)

$$Ar = \frac{d_p^3 \rho_g (\rho_s - \rho_g)g}{\mu^2}$$
 $a = \frac{K_2}{2K_1}$ $b = \frac{1}{K_1}$ (8)

The constants K_1 and K_2 are determined from the following equations which are based on the Ergun pressure drop equation for a bed of particles

$$K_1 = \frac{1.75}{\epsilon_{mf}^3 \phi} \qquad K_2 = \frac{150(1 - \epsilon_{mf})}{\epsilon_{mf}^3 \phi^2}$$
 (9)

where ϵ_{mf} is the bed void fraction (-) at minimum fluidization and ϕ is sphericity (-) of the bed particles. For this paper, three correlations based on the work of Ergun, Wen and Yu, and Grace were used to calculate U_{mf} . The Ergun approach applied the void fraction ϵ_{mf} and particle sphericity ϕ . The Wen and Yu approach utilized the experimental coefficients of a=33.7, b=0.0408 while the Grace approach used a=27.2, b=0.0408.

3.3 Pyrolysis kinetics

A pyrolysis kinetics scheme based on the work of Di Blasi was implemented to predict the conversion of biomass into gas, tar, and char products [2, 3]. Figure 4 gives an overview of the scheme and its reaction mechanisms. Reactions 1–3

represent the primary conversion of biomass while reactions 4–5 are secondary reactions that reduce tar yield at long residence times.

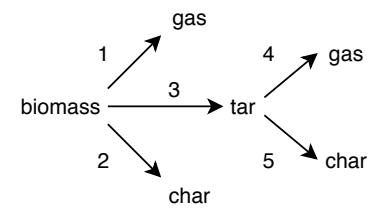


Figure 4: Diagram of the Di Blasi pyrolysis kinetics scheme for conversion of biomass to gas, tar, and char products.

The pyrolysis reactions were modeled as first-order Arrhenius type equations where the rate constant k for each reaction is given as

$$k = A e^{E/RT} (10)$$

such that A is the pre-factor, E is the activation energy, R is the gas constant, and T is the reaction temperature. Kinetic parameters for each reaction are listed in Table 1.

Table 1: Kinetic parameters for the Di Blasi biomass pyrolysis scheme.

Reaction	A (1/s)	E (kJ/mol)	Reference
1	4.38×10^{9}	152.7	[3]
2	3.27×10^{6}	111.7	[3]
3	1.08×10^{10}	148.0	[3]
4	4.28×10^{6}	108.0	[2]
5	1.00×10^{6}	108.0	[2]

3.4 Parameters

Parameters for the reduced-order model and CFD simulations are provided in Table 2. Biomass particle characteristics and properties are representative of loblolly pine. Bed particle characteristics are for typical sand material. Operating conditions and reactor dimensions are based on the previously discussed NREL 2FBR fluidized bed pyrolysis unit.

Table 2: Biomass, bed, and reactor modeling parameters. Particle diameters represent the Sauter-mean diameter.

10 the Sauter mean distinction.						
Parameter	Value	Units	Description			
$d_{p,\mathrm{bed}}$	235	μm	diameter of bed Particle			
$\phi_{ m bed}$	0.0		sphericity of bed particle			
$d_{p,\mathrm{bio}}$	135	$\mu\mathrm{m}$	diameter of biomass particle			
$\phi_{ m bio}$	0.0		sphericity of biomass particle			
$ ho_{ m bio}$	540	${ m kg/m^3}$	density of biomass particle			
$h_{reactor}$	43.18	cm	reactor height			
h_{static}	10.16	cm	static bed height			
${ m T}$	773	K	reactor temperature			

3.5 Simulation cases

Table 3 represents the CFD simulations conducted for this paper. Each row is for a different simulation case which is performed for a particular gas composition.

Table 3: Simulation cases for different gas mixtures where columns denote gas percentage.

Case	N_2	H_2	$\rm H_2O$	CO	CO_2	CH_4
1	100	0	0	0	0	0
2	0	100	0	0	0	0
3	0	0	100	0	0	0
4	0	0	0	100	0	0
5	0	0	0	0	100	0
6	0	0	0	0	0	100
7	20	20	0	20	20	20
8	50	0	0	0	50	0
9	50	0	0	50	0	0
10	0	0	50	50	0	0
11	100	0	0	0	0	0
12	80	20	0	0	0	0
13	60	40	0	0	0	0
14	50	50	0	0	0	0
15	40	60	0	0	0	0
16	30	70	0	0	0	0
17	20	80	0	0	0	0
18	15	85	0	0	0	0
19	10	90	0	0	0	0
20	5	95	0	0	0	0
21	0	100	0	0	0	0

4 Results and discussion

This section provides results and related discussions for the effects of different fluidization gases on the operation and conversion of a bubbling fluidized bed reactor.

4.1 Comparison of gas properties

Molecular weight, viscosity, density, and thermal conductivity of the individual gases investigated in this paper are shown in Figure 5. The gas properties were calculated at a pressure of 101,325 Pa and a temperature of 773.15 K (500°C). The lightest gas in terms of molecular weight and density is hydrogen while the heaviest gas is carbon dioxide. Viscosity for all the gases except hydrogen and methane ranged from 300–350 μP . Thermal conductivity for all the gases is near 0.05 W/(m K) except for hydrogen which is approximately 0.35 W/(m K) and methane which is near 0.12 W/(m K).

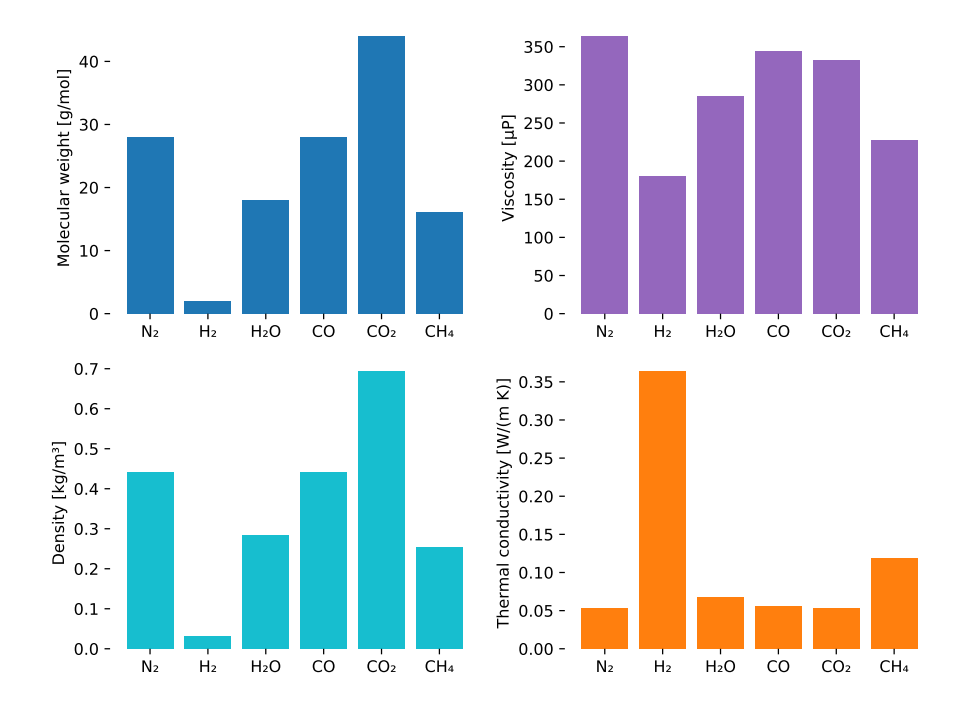


Figure 5: Comparison of molecular weight, viscosity, density, and thermal conductivity for individual gases at 101,325 Pa and 773.15 K.

Properties for molecular weight, viscosity, and density for the gas mixtures investigated in this paper are shown in Figure 6. Similar to the individual gas properties, the mixture properties were calculated at 101,325 Pa and 773.15 K

 (500°C) . The fraction of each gas in the mixture is given by the values shown at the top of each column in the figure. For example, the hydrogen and nitrogen mixture is comprised of 80% hydrogen and 20% nitrogen which is labeled as 0.8+0.2. As expected, the carbon dioxide mixture is the heaviest in terms of molecular weight and density.

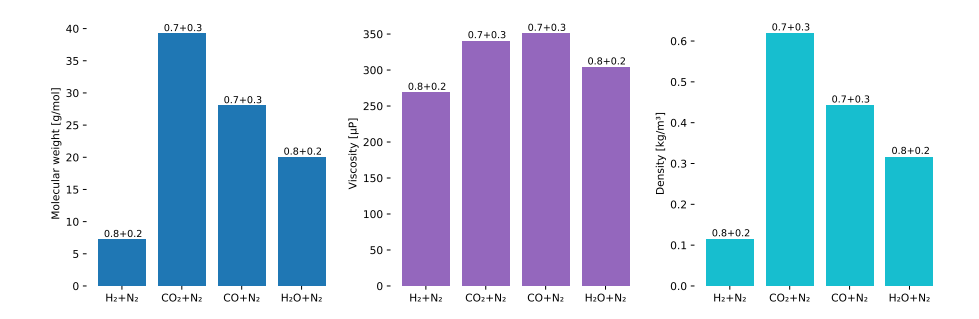


Figure 6: Comparison of gas mixture properties for molecular weight, viscosity, and density at 101,325 Pa and 773.15 K. Fraction of each gas component is shown at the top of each column.

4.2 Fluidization effects

Minimum fluidization velocity (Umf) of the bed material for the different fluidization gases is presented in Figure 7. The hydrogen gas requires about twice the gas velocity to fluidize the sand bed compared to the nitrogen gas.

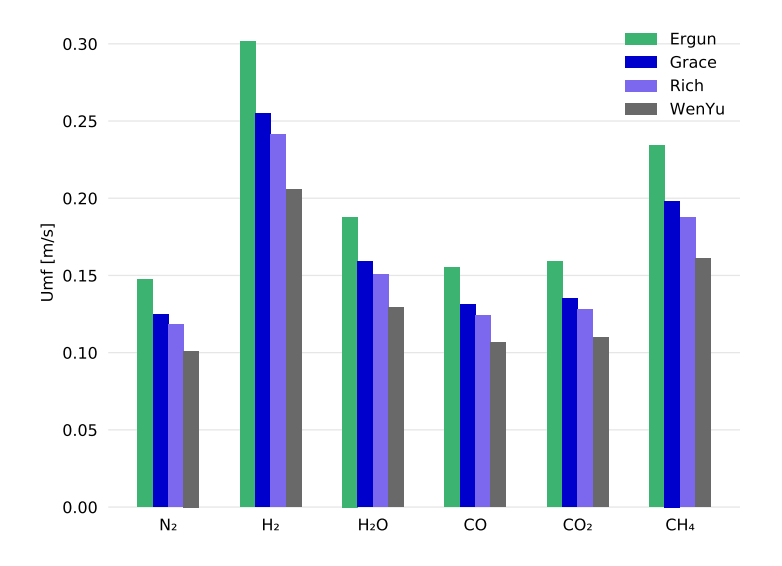


Figure 7: Comparison of minimum fluidization velocity (Umf) for different fluidization gases. Values calculated with the Ergun, Grace, and Wen and Yu correlations.

4.3 Evaluation of the kinetic scheme

The Di Blasi kinetics were put to use in a batch reactor model to investigate the time scales associated with the reaction mechanisms. Figure 8 is an overview of the biomass conversion and product yields using the Di Blasi kinetics in a batch reactor at 773.15 K (500°C). At this temperature, without the effects of secondary reactions, the kinetics offer a maximum achievable tar yield of 78% within 5 seconds. However, if secondary reactions occur during the entire pyrolysis process then a maximum tar yield of only 53% is possible. The Di Blasi kinetics suggest that minimizing the extent of secondary reactions is critical to producing the maximum possible tar yield.

A range of reaction temperatures were applied to the Di Blasi kinetics in the batch reactor model as shown in Figure 9. The kinetics suggest that temperature has a neglible effect on primary tar yield but effects of secondary reactions are more pronounced. When secondary reactions occur during the entire pyrolysis process, maximum tar yields are realized at higher temperatures but with shorter residence times. These results suggest that if secondary reactions are minimized then temperature should not have a drastic effect on tar yield.

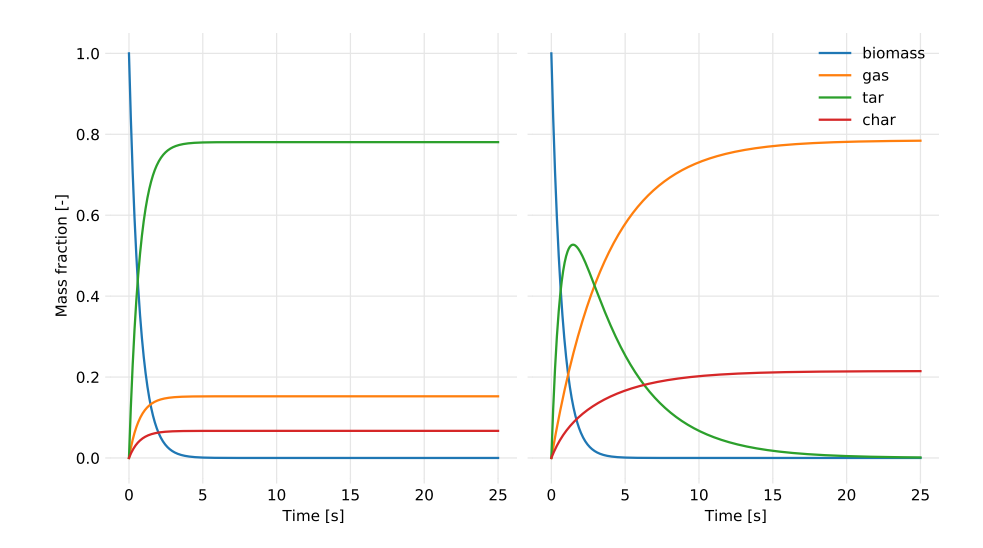


Figure 8: Biomass conversion and product yields in a batch reactor model at 773.15 K (500°C) according to the Di Blasi kinetic reactions. Results shown for primary reactions only (left) along with primary and secondary reactions (right).

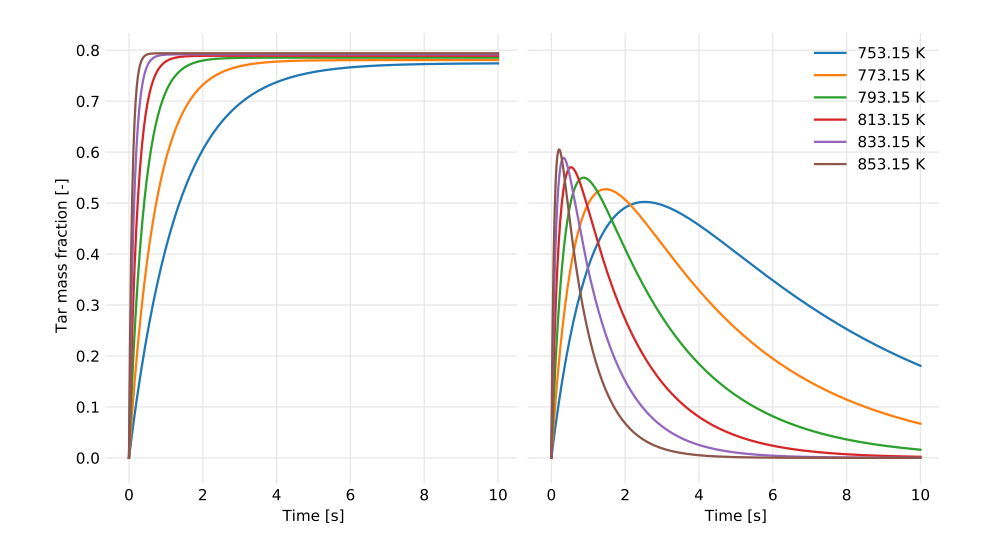


Figure 9: Tar yields for reaction temperatures of 753.15-853.15 K ($480-580^{\circ}$ C) using the Di Blasi kinetics in a batch reactor model. Results shown for primary tar (left) along with primary and secondary tar (right).

4.4 Solid and gas residence times

Here.

5 Conclusion

Here.

6 Source code

Python models used to generate results for this article are available on the CCPC GitHub at https://github.com/ccpcode in the X repository. Functionality provided by the Chemics package was used for gas properties and various fluidization calculations. See the Chemics documentation at https://chemics.github.io for more information.

References

- [1] M. Asadullah et al. "Jute stick pyrolysis for bio-oil production in fluidized bed reactor". In: *Bioresource Technology* 99 (2008), pp. 44–50.
- [2] Colomba Di Blasi. "Analysis of Convection and Secondary Reaction Effects Within Porous Solid Fuels Undergoing Pyrolysis". In: Combustion Science and Technology 90 (1993), pp. 315–340.
- [3] Colomba Di Blasi and Carmen Branca. "Kinetics of Primary Product Formation from Wood Pyrolysis". In: *Industrial & Engineering Chemistry* Research 40 (2001), pp. 5547–5556.
- [4] A.V. Bridgwater. "Principles and practice of biomass fast pyrolysis processes for liquids". In: *Journal of Analytical and Applied Pyrolysis* 51 (1999), pp. 3–22.
- [5] Tony Bridgwater. "Challenges and Opportunities in Fast Pyrolysis of Biomass: Part I". In: Johnson Matthey Technology Review 62.1 (2018), pp. 118–130.
- [6] Thomas Graham. "On the Motion of Gases". In: *Philosophical Transactions of the Royal Society of London* 136 (1846), pp. 573–631.
- [7] F. Herning and L. Zipperer. "Calculation of the Viscosity of Technical Gas Mixtures From the Viscosity of the Individual Gases". In: *Gas-und Wasserfac* 79 (1936), pp. 69–73.
- [8] Daniel Howe et al. "Field-to-Fuel Performance Testing of Lignocellulosic Feedstocks: An Integrated Study of the Fast Pyrolysis-Hydrotreating Pathway". In: *Energy & Fuels* 29 (2015), pp. 3188–3197.
- [9] Daizo Kunii and Octave Levenspiel. *Fluidization Engineering*. 2nd ed. Chemical Engineering. Butterworth-Heinemann, 1991.

- [10] Ofei D. Mante et al. "The influence of recycling non-condensable gases in the fractional catalytic pyrolysis of biomass". In: *Bioresource Technology* 111 (2012), pp. 482–490.
- [11] Pelle Mellin, Efthymios Kantarelis, and Weihong Yang. "Computational fluid dynamics modeling of biomass fast pyrolysis in a fluidized bed reactor, using a comprehensive chemistry scheme". In: Fuel 117 (2014), pp. 704–715.
- [12] Dinesh Mohan, Charles U. Pittman, and Philip H. Steele. "Pyrolysis of Wood/Biomass for Bio-oil: A Critical Review". In: *Energy & Fuels* 20 (2006), pp. 848–889.
- [13] Charles A. Mullen, Akwasi A. Boateng, and Neil M. Goldberg. "Production of Deoxygenated Biomass Fast Pyrolysis Oils via Product Gas Recycling". In: *Energy & Fuels* 27.7 (2013), pp. 3867–3874.
- [14] K. Papadikis, S. Gu, and A.V. Bridgwater. "Computational modelling of the impact of particle size to the heat transfer coefficient between biomass particles and a fluidised bed". In: *Fuel Processing Technology* 91 (2010), pp. 68–79.
- [15] Anna Trendewicz et al. "Evaluating the effect of potassium on cellulose pyrolysis reaction kinetics". In: *Biomass and Bioenergy* 74 (2015), pp. 15–25.
- [16] Huiyan Zhang et al. "Biomass fast pyrolysis in a fluidized bed reactor under N2, CO2, CO, CH4 and H2 atmospheres". In: *Bioresource Technology* 102 (2011), pp. 4258–4264.